Integration between ground based and satellite SAR data in landslide mapping: The San Fratello case study

Geomorphology 223 (2014) 45–60

Contents lists available at ScienceDirect

Geomorphology

journal homepage: www.elsevier.com/locate/geomorph

Integration between ground based and satellite SAR data in landslide mapping: The San Fratello case study

Federica Bardi [a,*], William Frodella [a], Andrea Ciampalini [a], Silvia Bianchini [a], Chiara Del Ventisette [a], Giovanni Gigli [a], Riccardo Fanti [a], Sandro Moretti [a], Giuseppe Basile [b], Nicola Casagli [a]

[a] Earth Science Department, Università di Firenze, via La Pira 4, Firenze 50121, Italy
[b] Dipartimento Regionale della Protezione Civile, Regione Siciliana, Servizio Rischi Idrogeologici e Ambientali, via Abela 5, Palermo 90141, Italy

ARTICLE INFO

Article history:
Received 5 February 2014
Received in revised form 12 June 2014
Accepted 13 June 2014
Available online 6 July 2014

Keywords:
Satellite interferometry
Ground-based radar
PSI
Landslide mapping
Ground deformation
SAR data integration

ABSTRACT

The potential use of the integration of PSI (Persistent Scatterer Interferometry) and GB-InSAR (Ground-based Synthetic Aperture Radar Interferometry) for landslide hazard mitigation was evaluated for mapping and monitoring activities of the San Fratello landslide (Sicily, Italy). Intense and exceptional rainfall events are the main factors that triggered several slope movements in the study area, which is susceptible to landslides, because of its steep slopes and silty–clayey sedimentary cover.

In the last three centuries, the town of San Fratello was affected by three large landslides, developed in different periods: the oldest one occurred in 1754, damaging the northeastern sector of the town; in 1922 a large landslide completely destroyed a wide area in the western hillside of the town. In this paper, the attention is focussed on the most recent landslide that occurred on 14 February 2010: in this case, the phenomenon produced the failure of a large sector of the eastern hillside, causing severe damages to buildings and infrastructures. In particular, several slow-moving rotational and translational slides occurred in the area, making it suitable to monitor ground instability through different InSAR techniques.

PS-InSAR™ (permanent scatterers SAR interferometry) techniques, using ERS-1/ERS-2, ENVISAT, RADARSAT-1, and COSMO-SkyMed SAR images, were applied to analyze ground displacements during pre- and post-event phases. Moreover, during the post-event phase in March 2010, a GB-InSAR system, able to acquire data continuously every 14 min, was installed collecting ground displacement maps for a period of about three years, until March 2013. Through the integration of space-borne and ground-based data sets, ground deformation velocity maps were obtained, providing a more accurate delimitation of the February 2010 landslide boundary, with respect to the carried out traditional geomorphological field survey. The integration of GB-InSAR and PSI techniques proved to be very effective in landslide mapping in the San Fratello test site, representing a valid scientific support for local authorities and decision makers during the post-emergency management.

1. Introduction

Landslide mapping in the field is often a quite complex task; this can be owing to (i) the size of the landslide, often too large to be completely observed in the field; (ii) the viewpoint of the investigator, often inadequate to see all parts of a landslide (e.g., the scarp, lateral edges, deposit, toe) with the same detail; or (iii) the fact that old landslides are often partially or totally covered by vegetation or have been partly dismantled by other landslides, erosion processes, and human actions, including agricultural and forest practices (Guzzetti et al., 2012). The reduced visibility of the slope failure makes it difficult to accurately follow a landslide boundary in the field: this is a consequence of the local perspective of the size of the landslide and of the fact that the landslide boundary is often indistinct.

Thus, the perspective offered by a distant view of the landslide is preferable and can result in more accurate and more complete landslide mapping (Guzzetti et al., 2012).

In this paper, an improvement of the 2010 San Fratello landslide map was performed through the use of radar interferometry, specifically integrating the Persistent Scatterer Interferometry (PSI) with the Ground-based Synthetic Aperture Radar Interferometry (GB-InSAR).

The PSI is a well-known powerful and advanced multitemporal interferometric SAR technique, which allows measuring centimetric and subcentimetric ground displacements occurring during a defined range of time with millimeter accuracy (Ferretti et al., 2001). This work fully exploits both the satellite systems operating in the microwave C-band (i.e., ERS 1/2, ENVISAT, and RADARSAT-1 interferometric archives) and

* Correspondig author at: via La Pira 4, Firenze 50121, Italy. Tel.: +39 055 2757777; fax: +39 055 2757788.
E-mail address: federica.bardi@unifi.it (F. Bardi).

http://dx.doi.org/10.1016/j.geomorph.2014.06.025

new generation SAR data acquired in X-band by the recent space missions, such as COSMO-SkyMed. The analysis of the benefits introduced by the aforementioned new satellite missions, in terms of technical performances and improvements in applications, was here investigated.

The GB-InSAR is a powerful terrestrial technique, widely used in engineering and in geological applications to detect the target (structure and ground) displacements (Casagli et al., 2002; Tarchi et al., 2003a; Noferini et al., 2007; Casagli et al., 2009; Herrera et al., 2009; Casagli et al., 2010; Del Ventisette et al., 2011). A GB-InSAR is a ground-based system that works with the same principles as space-borne sensors for monitoring ground deformation phenomena.

The interferometric technique is based on a comparison between two SAR images acquired at different times; this permits evidence of eventual displacements occurring during the time span between the two acquisitions. The time necessary to the sensor to realize two subsequent acquisitions is connected to the range of displacement velocities that the instrument can recognize. Therefore, satellite data are useful in monitoring extremely or very slow movements, whereas the GB-InSAR devices allow the assessment of ground deformations of faster landslides, thanks to the possibility of realizing higher frequency measurements (Corsini et al., 2006; Noferini et al., 2008). In addition, the spatial coverage of satellite data is limited by the SAR imaging geometry caused by layover, foreshortening and shadowing effects (Ferretti et al., 2001). A GB-InSAR, on the other hand, also can be placed in front of steep slopes, which are in most cases not visible from space-borne platforms.

The PSI and GB-InSAR work at different spatial and temporal scales. Because of the above-mentioned characteristics and differences, the integration of these techniques enables us to obtain useful information on the ground displacement measurements, with high precision and improved spatial and temporal resolution. In particular, the use of PSI allows performing a preliminary study on ground displacements at a basin scale, providing hotspot mapping (which can be useful prior to planning a GB-InSAR system installation for a monitoring campaign) over a specific area affected by landslides.

Between the end of 2009 and the beginning of 2010, the Nebrodi Mountains (western Sicily, Italy) were highly affected by several landslide events causing intense damages and casualties. Some of these landslides are still active at present day. Intense and exceptional rainfall events (about 900 mm in the period between October 2009 and January 2010) were the main factor that, combined with the strong topographical relief, triggered several slope movements. In this work, the PSI and GB-InSAR techniques were qualitatively integrated in order to improve the 2010 landslide map. The satellite data, measured along the satellite Line Of Sight (LOS), were projected on the slope direction, providing the component of the velocity registered by the sensors on the direction of the slope (V_{slope}). The line of sight of the GB-InSAR system is quite similar to the slope direction, so the displacements registered in this direction are comparable to the projected satellite data.

A list of the used satellite data is shown in Table 1 together with the characteristics of the sensors. The GB-InSAR data were recorded during the monitoring campaign, realized between March 2010 and March 2013: in this period the instrument generated interferograms continuously, every 14 min.

The integration was based on a binary approach to divide the areas characterized by displacements from the ones without displacements. The method was validated comparing the results with the evidence of the damage assessment map produced by the Department of Civil Protection (Fig. 5) and on the basis of the results of field trips, which allowed us to detect soil fractures and landslide scarps (Figs. 4C and 5). The integration was used to update the map of the San Fratello landslide.

2. Geomorphological and geological framework

The town of San Fratello is located in northeastern Sicily, Italy (Messina Province, Fig. 1B), on the northwestern hillside of the Nebrodi Mountains (Fig. 1A), a 70-km-long ridge with an ENE–WSW direction, within the southern Apennine chain.

The geomorphology of the study area shows the typical features of the Sicilian Tyrrhenian coastline: steep slopes rise abruptly from the coastal plain and are deeply cut by N–NW-directed creek valleys (called *fiumare*). In this context, the town of San Fratello is located about 5 km south of the seaside, on a divide separating the Furiano Creek valley to the west from the Inganno Creek valley to the east (Fig. 1C).

From a geological point of view, the study area is part of the northeastern sector of the Apennine–Maghrebian orogenic belt, and it is characterized by the tectonic overriding of the uppermost Kabilian-Calabrid units, consisting of dolomitic limestones and sandstones (Fig. 2A, B), formed in this area mainly by marlstone and claystone formations (Ogniben, 1960; Atzori and Vezzani, 1974; Lentini and Vezzani, 1975; Atzori et al., 1978; Lentini et al., 1990, 1994, 1995; Finetti et al., 1996; Lentini et al., 2000). This geological framework determines the overlapping of geological formations with marked differences in geotechnical properties, deeply influencing the study area landscape and slope instability phenomena: hilltops, made of hard-brittle lithologies, are undermined by the weathering and erosional processes taking place in the underlying soft clayey formations. In the San Fratello area, on the top of the bedrock, a silty–clayey cover lies with an average thickness of about 10 m; the 2010 landslide affected this layer, involving all the thickness or the biggest part of it, with a surface rupture 8–10 m deep (Pino et al., 2010). The low quality of the geotechnical properties of this layer probably played an important role in the landslide trigger, together with the steep slope angle (more than 30°) and the intense precipitation events of the period. In particular, the period between October 2009 and January 2010 recorded more than 900 mm of precipitation (Fig. 3). The area was impacted by other similar phenomena in the past; in 1754, a large landslide damaged the northeastern sector of

Table 1
Characteristics of the satellites used for the PS-InSAR monitoring of the San Fratello landslide.

Satellite	ERS 1/2	ERS 1/2	ENVISAT	ENVISAT	RADARSAT-1	RADARSAT-1	COSMO-SkyMed
Band	C	C	C	C	C	C	X
Geometry	Ascending	Descending	Ascending	Descending	Ascending	Descending	Descending
Repeat time (days)	35	35	35	35	24	24	4
Temporal range	11/09/92–05/06/00	01/05/92–08/01/01	22/01/03–22/09/10	07/07/03–13/09/10	30/12/05–04/09/09	31/01/06–06/10/09	16/05/11–02/05/12
N° scenes	34	70	65	49	46	47	32
PS/km^2	6.55	2.25	64.74	20.41	112.73	86.86	400.62
Spatial accuracy (m)	±4–±10	±4–±10	±4–±10	±4–±10	±4–±8	±4–±8	±3
0 ± dev. stand. (mm/y) (0 ± σ)	0 ± 2.5	0 ± 1.7	0 ± 2.1	0 ± 1.5	0 ± 2.5	0 ± 2.1	0 ± 3.7
LOS vel. range (min, max) (mm/y)	−9.5, +7.2	−26.8, +8.6	−39.3, +10.1	−22.5, +5.9	−46.8, +19.8	−26.3, +20.5	−56.4, +31.8
Mean LOS vel. (mm/y)	−0.5	−0.4	0.0	−0.6	−0.4	0.0	−1.0

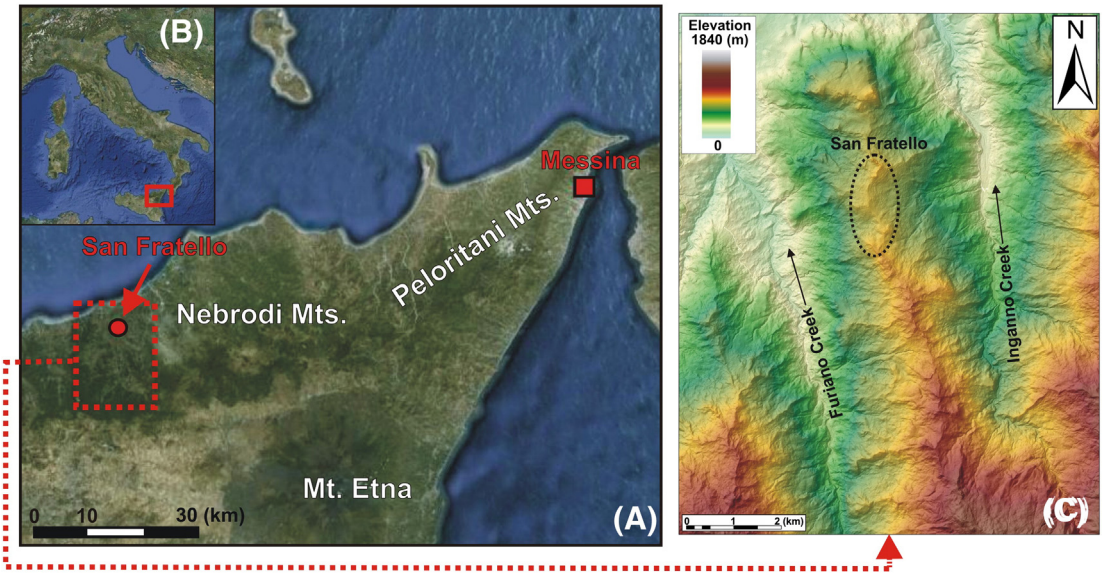

Fig. 1. Geographic framework (A–B) and digital elevation model (C) of the San Fratello area.

the town; in 1922 a wide area in the western hillside of the town was completely destroyed by another landslide (Fig. 4A). In Fig. 4B, the landslide inventory map (PAI, Hydrogeological Setting Plan databases) of the area is shown; it was performed before the 2010 collapse and confirmed the existence of a large, dormant, complex, landslide phenomena as well as several other smaller, active, and shallow-seated mass movements.

The 14 February 2010 landslide (Fig. 4) represents the most recent event, causing the failure of a large sector of the eastern hillside, inducing severe damages to buildings and infrastructures, in particular in the quarters of Stazzone, Riana, Porcaro, and San Benedetto (Bianchini et al., 2014) (Fig. 4C).

In detail, the 2010 landslide, affecting an area of about 1 km^2, developed from the eastern sector of the town area toward the Inganno Creek valley for a length of about 1.8 km (Fig. 4C). This landslide, mainly involving the silty–clayey overlay, is a complex rotational mass movement that intensively modified the topographic slope surface, producing multiple failures, traction cracks, and counterslopes (Fig. 4C). On this geomorphological map, some kinematic indicators are represented, emphasizing the direction of the flow toward the valley of Inganno Creek (Fig. 4C); the areas characterized by ground and building lacerations were also pointed out, together with the damaged drain pipelines and the hydrographic network that was intensely modified, producing concentrated runoff and several small landslide lakes. The landslide, in its lower sector, evolved in an earth flow, channelizing into a stream bed corresponding to a tributary of the Inganno Creek.

An overview of the building damages and of the fracture pattern is represented in Fig. 5.

In particular, the landslide main scarps, characterized by heights between 5 and 10 m, are located in the middle and upper part of the slope about 500 m east of the town center (Fig. 5D, correspondent to sector 1, Porcaro quarter, in Fig. 4C). In this latter sector, where the ground surface planar translation reached 50 m, severe damages to some isolated buildings and local roads occurred. In the eastern town sector, characterized by a high building density, translational sliding phenomena determined subparallel fracture systems and scarps in the Riana quarter (sector 3 in Fig. 4C), while in correspondence with the Stazzone quarter (sector 2 in Fig. 4C), rotational phenomena induced several extensional and compressive fractures (Fig. 5). In both quarters, several buildings were intensively damaged (e.g., the church and the primary school in the Stazzone quarter in particular, Fig. 5A) or completely destroyed together with the sewer system. The southern town sector (San Benedetto quarter, sector 4 in Fig. 4C) was affected by translational and rotational phenomena, which induced intense ground laceration and formed scarps up to 5 m high, destroying several buildings (Fig. 5C), water pipes, and roads. The upper part of the town, in correspondence with the divide (sector 5 in Fig. 4C), was also affected by intense ground deformation phenomena (Fig. 5B).

3. Methodology

The InSAR techniques, applied from space-borne and ground-based platforms, have proven to be a powerful tool in the field of ground displacement analysis, thanks to their high spatial and temporal resolution as well as all-weather capability (Massonnet and Feigl, 1998; Singhroy et al., 1998; Crosetto et al., 2011).

Radar techniques are an example of active remote sensing: radar sensors emit a microwave radiation in order to scan objects and areas, recording the reflecting or backscattering radiation of the target. The SAR interferometry techniques are based on the evaluation of the phase difference (interferometric phase) between two or more acquisitions of SAR images, enabling us to detect movements along the Line Of Sight (LOS) (Tarchi et al., 1997; Antonello et al., 2004; Crosetto et al., 2005). In the absence of errors caused by the propagation of the radar signal in the atmosphere, to the pixel scattering, and to the instrumental and geometrical decorrelation, the lag owing to the propagation is proportional only to the distance between the sensor and the target. When a displacement occurs in the elapsing time between two acquisitions, the interferometric phase will vary accordingly. The SAR interferometry uses this effect in order to measure ground deformation (Ferretti et al., 2000). Because of the ambiguous nature of the 2π interferometric phase-wrapping, a quarter of the wavelength represents the maximum displacement that can be recorded between two successive acquisitions; this effect is called *aliasing* and it represents one of the main limitations of the technique applications (e.g., Hanssen, 2005; Crosetto et al., 2010).

3.1. PSI technique

Space-borne InSAR is an effective technique for ground deformation measurements over large areas, ideal for monitoring subvertical displacements of the ground surface characterized by low velocity. The principal limitations of the classical DInSAR (Differential Interferometric SAR) techniques are caused by temporal and geometrical decorrelation

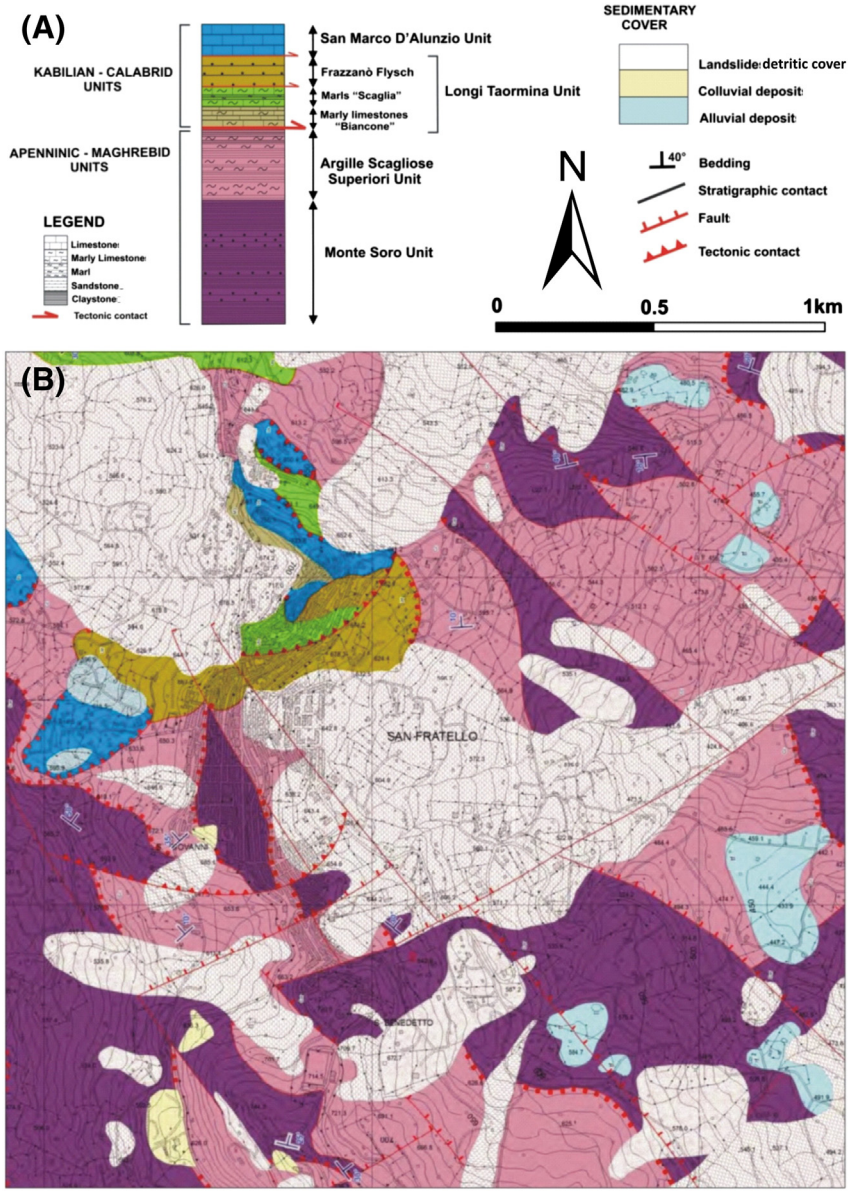

Fig. 2. Tectono-stratigraphic section (A) and geological map (B) of the San Fratello area (modified after Pino et al., 2010).

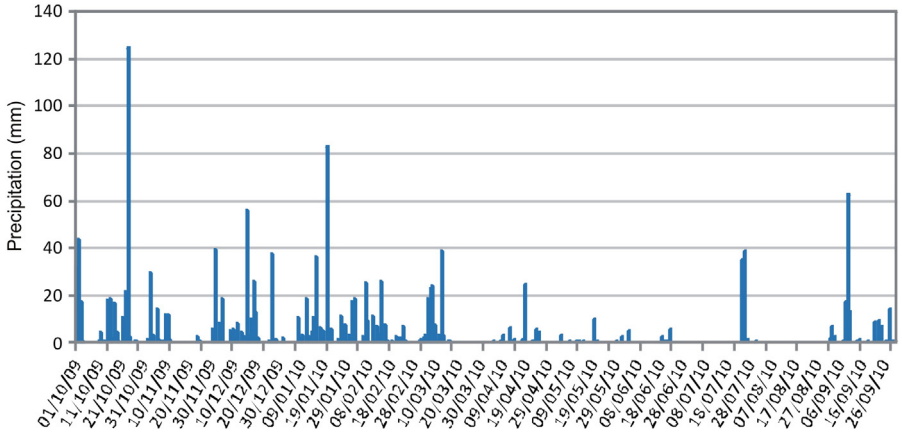

Fig. 3. Daily precipitation value (mm) registered in the San Fratello area between October 2009 and October 2010.

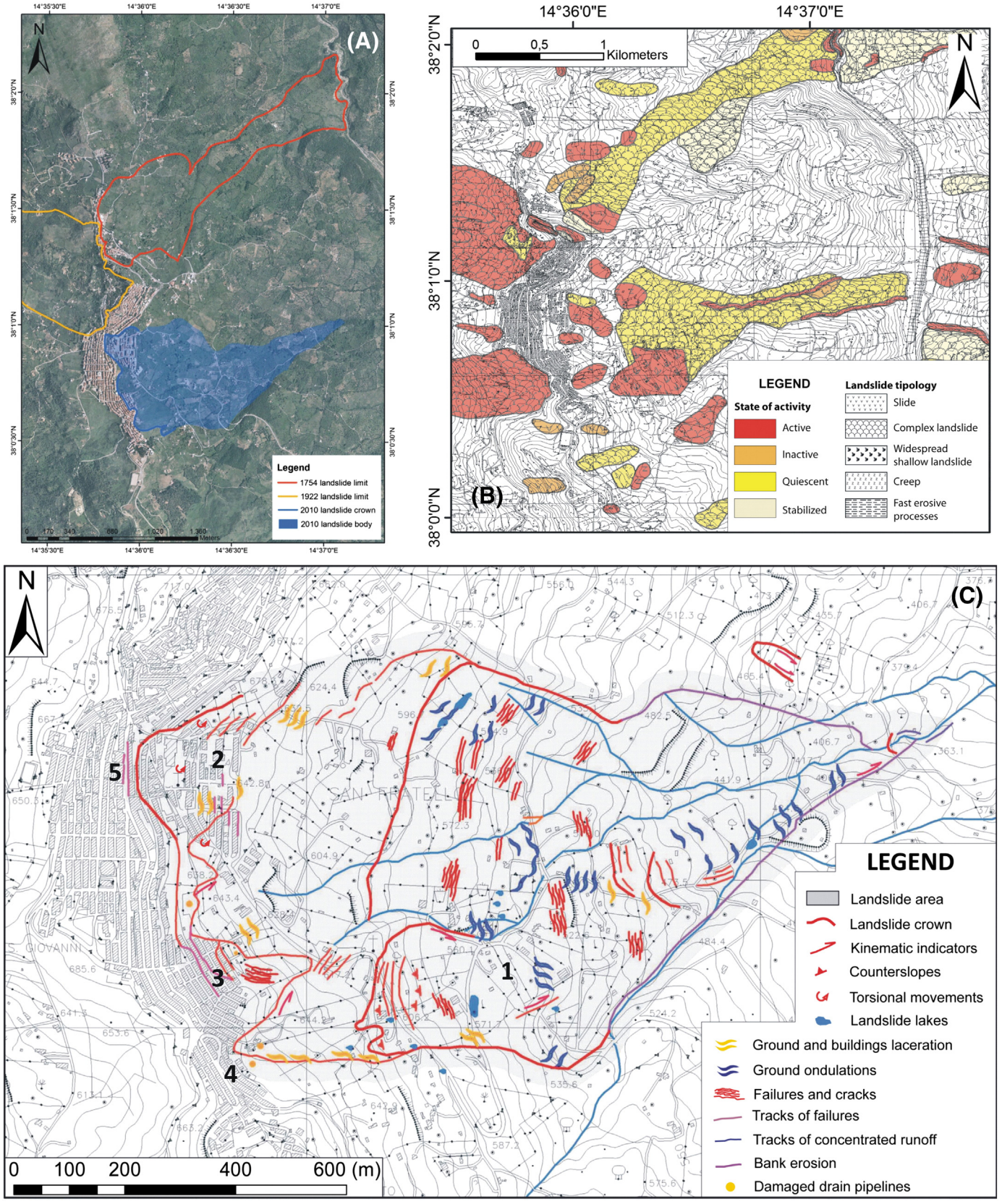

Fig. 4. (A) The three landslides affecting San Fratello: the 1754 landslide in red, the 1922 landslide in yellow and the 2010 landslide in blue. (B) Inventory landslide map of the San Fratello area (PAI, 2010). (C) Geomorphological map of the 2010 landslide (Pino et al., 2010). San Fratello quarters: 1, Porcaro; 2, Stazzone; 3, Riana; 4, S. Benedetto; and 5, Latteri Street. (For interpretation of the references to color in this figure legend, the reader is referred to the web version of this article.)

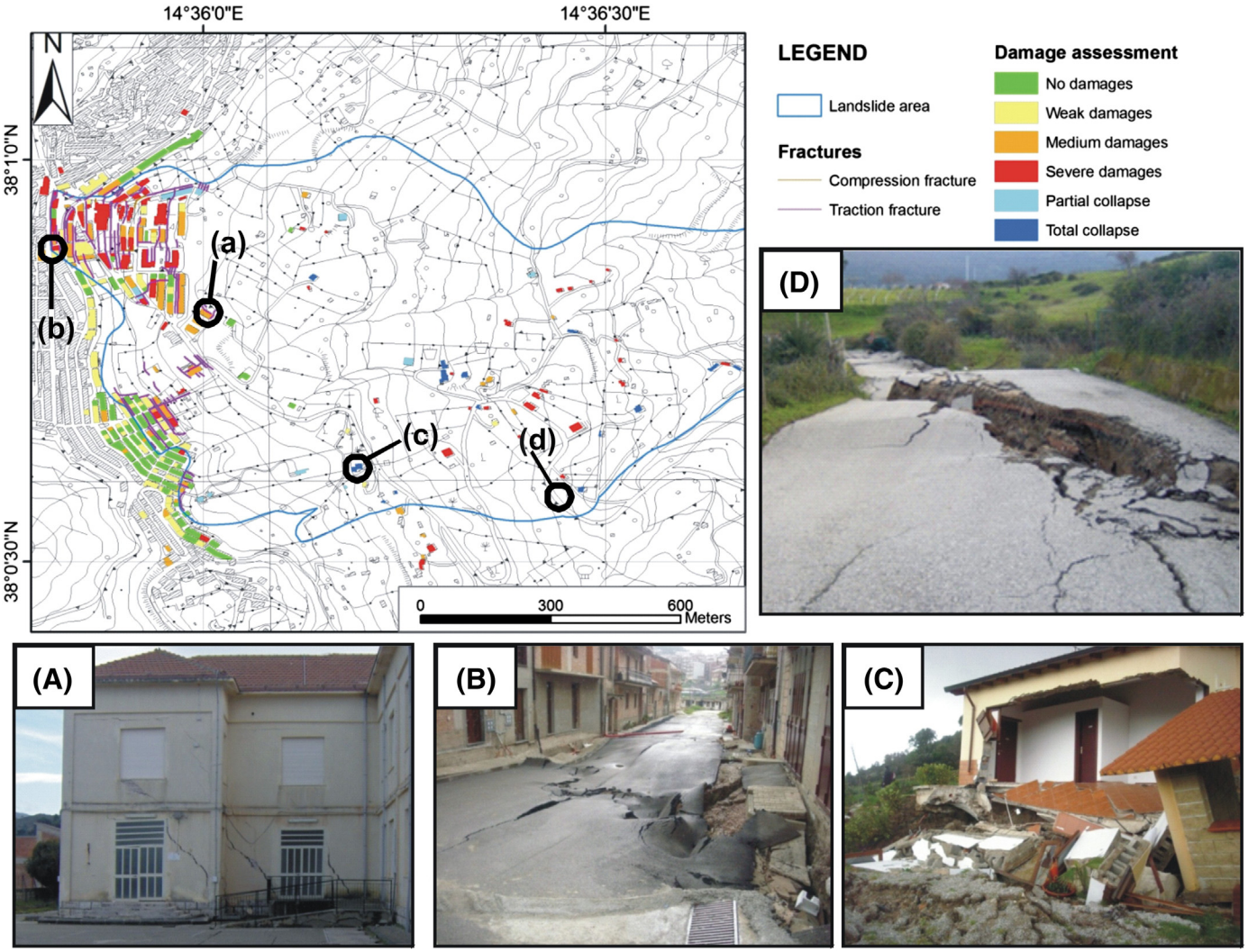

Fig. 5. Building damage and fracture pattern maps (courtesy of the Regional Civil Protection Department, Sicily) and example of ground deformations and damages to buildings and structures in the 2010 landslide area (A, structural damages to the primary school building, Stazzone Quarter; B, damages to the pavement of Latteri Street; C, building failure in San Benedetto quarter; D damages to local road in Porcaro Quarter).

and atmospheric noises (Colesanti et al., 2003). On the contrary, the multi-interferogram approach, such as the PS-InSAR™ technique (Ferretti et al., 2001), obtains a precise ground deformation map on a sparse grid of phase-stable radar targets (the so-called permanent scatterer, PS). The PS targets correspond mainly to man-made (monuments, metallic structures) or natural objects (such as rock outcrops) that are stable and coherent scatterers (Ferretti et al., 2000). Therefore, urbanized zones and cities are characterized by a high PS density; whereas, within vegetated, rural, and forested areas, benchmarks are very few and PSI tends to occasionally fail. Satellites follow near-polar orbits and are rightward side-looking. Thus, in ascending orbit, the LOS of the satellite is oriented toward the east, and it is more useful to detect the displacements that occur in this direction. On the contrary, the descending orbit satellites are more suitable for the observation of west-facing slopes.

The PS-InSAR™ technique is able to identify the PS displacement as the only contribution to the signal phase shift, until the aliasing effect is negligible; this technique permits us to have a long temporal series of SAR data. Multiple differential interferograms obtained from a set of radar scenes, acquired on the same track, provide displacement measurements with high precision. Specifically, the precision on the average LOS deformation rate is about 0.1–1 mm/y; while on the displacement time series a single measure is 1.5 mm/y (Ferretti et al., 2000, 2001, 2005; Hanssen, 2005; Raucoules et al., 2008; Crosetto et al., 2010). Accordingly, this technique has been successfully applied in the field of geology (e.g., subsidence, earthquakes, volcanic activities) for scientific studies and for hazard and risk assessment strategies (Farina et al., 2004; Meisina et al., 2008; Cigna et al., 2011; Pulvirenti et al., 2011; Bianchini et al., 2012; Ciampalini et al., 2012; Cigna et al., 2012; Raspini et al., 2012; Zhao et al., 2012; Del Ventisette et al., 2013; Ciampalini et al., 2014). Within the study area, in order to produce ground deformation velocity maps, the following satellite SAR data were employed: ERS 1/2, ENVISAT (European Space Agency), and RADARSAT-1 (Canadian Space Agency) data, provided by the Italian Civil Protection Department (DPC), and COSMO-SkyMed (Italian Space Agency) data. Satellite SAR frames cover areas up to 100 km^2, with resolutions of a few meters. The revisiting time of the present satellites over the same area ranges between 4 and 35 days. In Table 1, more information about the revisiting time, the temporal range and the number of available satellite scenes, the PS density, and the spatial accuracy of the SAR data are recorded; statistical data about the records of the satellites are also included in Table 1.

The ERS 1/2, ENVISAT, and RADARSAT-1 data stack in descending and ascending orbits and the COSMO-SkyMed in descending orbit has been processed by Tele-Rilevamento Europa (TRE) using SqueeSAR™, which represents the evolution of the PS-InSAR™ technique (Ferretti

et al., 2001, 2011). For measuring ground displacements, this new advanced multitemporal interferometric technique uses permanent scatterers and the so-called distributed scatterers (DS), which correspond to homogeneous areas spread over a group of pixels in a SAR image (rangeland, pasture, shrubs, and bare soils). The SqueeSAR™ technique increases the density of the point targets that register ground motion with respect to the traditional PS-InSAR™ technique, and it is very useful in the case of sparse vegetation landscapes (Meisina et al., 2013; Raspini et al., 2013; Bellotti et al., 2014). As recorded in Table 1, the ERS 1/2, ENVISAT, and RADARSAT 1 satellites acquired in C-band (COSMO-SkyMed uses the X-band data) that improves the level of detail of the investigation and the PSI capability for landslide mapping and monitoring. Indeed, the X-band satellites produce a new generation of SAR data, characterized by shorter revisiting time and higher spatial and temporal resolution with respect to C-band satellites, that can represent an effective tool for rapid updating of landslide inventory maps and for hazard and risk studies (Crosetto et al., 2010; Bovenga et al., 2012; Frattini et al., 2013). Regarding the aliasing effect, velocities compromising the PSI processing depend on the employed SAR microwave length and on the satellite repeat cycle: they are about 15 cm/y for ERS/ENVISAT data (C band), 21 cm/y for RADARSAT (C-band), and about 70 cm/y for COSMO-SkyMed (X-band).

As the 2010 landslide affected the east-facing slope, the best information about displacement was obtained from data stacks in ascending orbit. On the other hand, the descending orbit acquisition was more useful to identify recent displacements of the historical 1922 landslide, which took place on the west-facing slope. Considering the limitation related to the vegetation cover and in correspondence with the central and lower parts of the 2010 landslide, the highest number of PS was located in correspondence with the San Fratello town area, where the crown of both landslides was located.

3.2. GB-InSAR technique

In recent years, the GB-InSAR has proven to be a reliable and consistent technique for landslide monitoring applications (Luzi et al., 2004; Casagli et al., 2010; Gigli et al., 2011). A GB-InSAR system consists in a computer-controlled microwave transceiver, characterized by a transmitting and receiving antenna that, by moving along a mechanical linear rail, is able to synthesize a linear aperture along the azimuth direction. The transmitting antenna produces step-by-step continuous waves at discrete frequency values, sweeping a specific bandwidth generally in Ku band. A SAR image contains amplitude and phase information of the observed objects backscattered echo within the investigated scenario, and it is obtained by combining the spatial resolution along the direction perpendicular to the rail (range resolution, ΔRr) and the one parallel to the synthetic aperture (azimuth or cross-range resolution, ΔRaz) (Luzi et al., 2010). The working principle of the GB-InSAR technique is the evaluation of the phase difference, pixel by pixel, between two pairs of averaged sequential SAR complex images, which constitutes an interferogram (Bamler and Hartl, 1998). The latter does not contain topographic information, given the antennas fixed position during different scans (zero baseline condition); therefore, in the time elapsed between the acquisition of two or more subsequent coherent SAR images, it is possible to derive from the obtained interferogram a map of the displacements that occurred along the sensor LOS with a millimeter accuracy in the Ku band (Tarchi et al., 1997, 2000; Pieraccini et al., 2000a,b, 2003). Specifically, using ground-based platforms it is also possible to obtain centimetric spatial resolution with an accuracy of <0.5 mm. According to the specific acquisition geometry, only this component of the real displacement vector can be estimated, whereas the displacements that occurred along a direction perpendicular to the LOS are missed. This is one of the limitations of the GB-InSAR technique. The radar system must be placed in order to make the sensor LOS as parallel as possible to the expected direction of the landslide motion. Nevertheless, the GB-InSAR represents a versatile and flexible technology, allowing rapid changes in the type of data acquisition, such as geometry and temporal sampling, based on the characteristics of the monitored slope failure.

In the post-event phase, in order to monitor the San Fratello 2010 landslide and to assess its residual risk, a GB-InSAR system was set up on the left flank of the Inganno Creek valley in the Sanguinera village area opposite the San Fratello town (Fig. 6). The instrument was installed on 8 March 2010 and it started to acquire data two days later. The employed system is a ground-based SAR, designed and implemented by the Joint Research Centre (JRC) of the European Commission and its spin-off company Ellegi-LiSALab (Tarchi et al., 2003a,b; Antonello et al., 2004; Casagli et al., 2009, 2010; Gigli et al., 2011; Del Ventisette et al., 2012a,b; Tapete et al., 2012; Di Traglia et al., 2013; Intrieri et al., 2013). The radar system was installed at an average distance of 2100 m with respect to the landslide (Fig. 6). The area covered by a GB-InSAR system depends on this distance, which is usually limited to a few hundreds of meters up to a few kilometers, corresponding to a patch-landscape scale. In the specific case of San Fratello, the covered area is about 1 km^2, like the landslide extension. The accurate displacement maps can be produced only for the upper part of the landslide because the vegetated part is not visible by the GB-InSAR.

The radar parameters used during the measurement campaign are summarized in Table 2. Regarding the aliasing effect, it reduces to 4.4 mm the maximum displacement that can be recognized without ambiguity using the system installed on the test site. Contrary to the satellite systems, the *repeat cycle* of the GB-InSAR instruments is characterized by higher frequency; in the case of San Fratello, the measures were acquired every 14 min: during the monitoring period the displacements never exceeded the threshold of 4.4 mm in 14 min, so the aliasing effect was avoided.

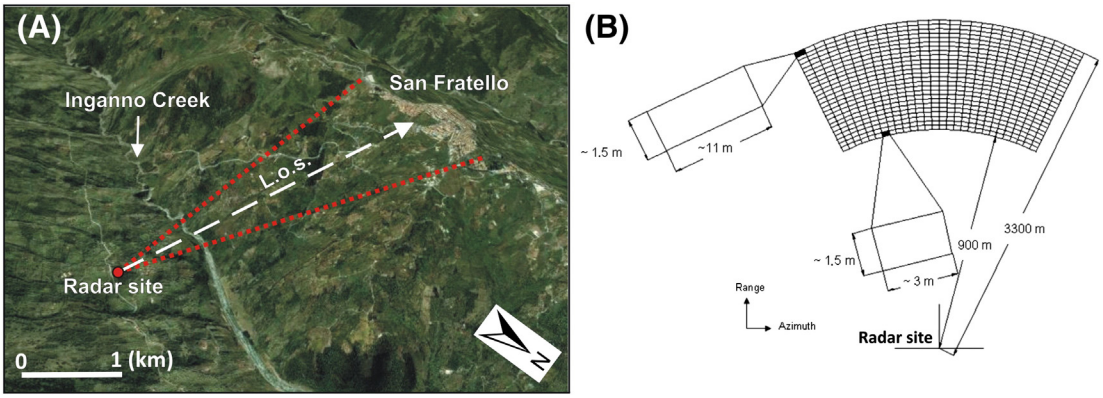

Fig. 6. Location of the San Fratello GB-InSAR system installation (A) and resolution grid size and parameters used during the monitoring campaign (B).

Table 2
GB-InSAR system parameters used to monitor the San Fratello landslide.

Central frequency	Band width	Synthetic aperture	Min. distance	Max. distance	ΔRr	ΔRaz (at 900-m distance)	ΔRaz (at 3300-m distance)	Scanning time
17.1 GHz	200 MHz	3.00 m	900 m	3300 m	1.5 m	3 m	11 m	14 min

3.3. Data integration

Regarding the San Fratello 14th February 2010 landslide, the displacements were studied during the pre- and post-event by the integration between space-borne and ground based InSAR techniques. The integration methodology is schematically described in Fig. 7 and consisted of three principal steps: the data collection, the SAR data post-processing, and the pre- and post-event data integration. During the data collection phase, geological and geomorphological field surveys were realized together with the acquisition of ancillary data (i.e., an orthophoto of the study area, landslide inventory map PAI databases, 2010, damage assessment map). Then satellite and ground-based SAR data were collected, covering a period of pre- (ERS 1/2, ENVISAT, RADARSAT-1) and post-event (COSMO-SkyMed and GB-InSAR). During the second step, the SAR data post-processing was performed: in order to increase the comparability of the different data sets, the satellite data were projected along the slope direction, which is quite similar to the GB-InSAR LOS; the procedure used for the projection is the same described in Colesanti and Wasowski (2006) and later in Bianchini et al. (2013) and in Herrera et al. (2013). The downslope projected velocity is called V_{slope}. Ground deformation velocity (V_{slope}) maps were obtained and superimposed on the orthophoto (characterized by a 1-m geometric resolution) and compared with the available landslide delimitation, performed a few days after the event, on the basis of the field evidences (geomorphological surveys and building damage assessment; Figs. 4C and 5).

To classify the PSI data, a stability V_{los} threshold at ±2 mm/y for C-band data was considered. This threshold is based on several published PSI analyses on landslide studies (e.g., Righini et al., 2012; Herrera et al., 2013).

In the study area, the velocity ranges of PSI data measured by the different satellite systems are comparable for all the PS populations: all the maximum (positive) and minimum (negative) velocity values range within a few tens of millimeters per year. The C-band data show a standard deviation of the velocity of about 2.0. The X-band PSI data have a slightly higher standard deviation (3.7) than C-band. This feature mainly depends on the number and distribution of SAR scenes used for the processing over the temporal acquisition period. Nevertheless, in our case, X-band COSMO-SkyMed data set includes a sufficient number of images (i.e., 32 images) homogeneously distributed over one year acquisition. Considering this characteristic, the same stability threshold value (±2 mm/y) has been used for C-band and for X-band data in order to make all the used PSI data acquired by different satellite sensors as comparable as possible. Moreover, this value is acceptable as it does not exceed the precision of the PSI technique.

To classify V_{slope} data, the same statistical considerations were taken into account, considering the negative skewness of the V_{slope} PS population. So the V_{slope} positive data that represent outliers in the distribution are negligible, and therefore the V_{slope} stability value is chosen between 0 and −2 mm/y. Statistical data of the PSI data sets are displayed in Table 1.

At the same time, GB-InSAR data were analyzed to obtain displacement maps and time series of 10 stable points, chosen in areas where the radar signal is characterized by high stability, high signal/noise ratio, and high power and coherence parameters.

The third step is defined *data integration* and consisted of the qualitative integration between space-borne V_{slope} maps and ground-based displacement maps; the integration was based on a binary approach to identify the areas characterized by displacements to the ones without evidence of movement, during the pre- and post-event period. The

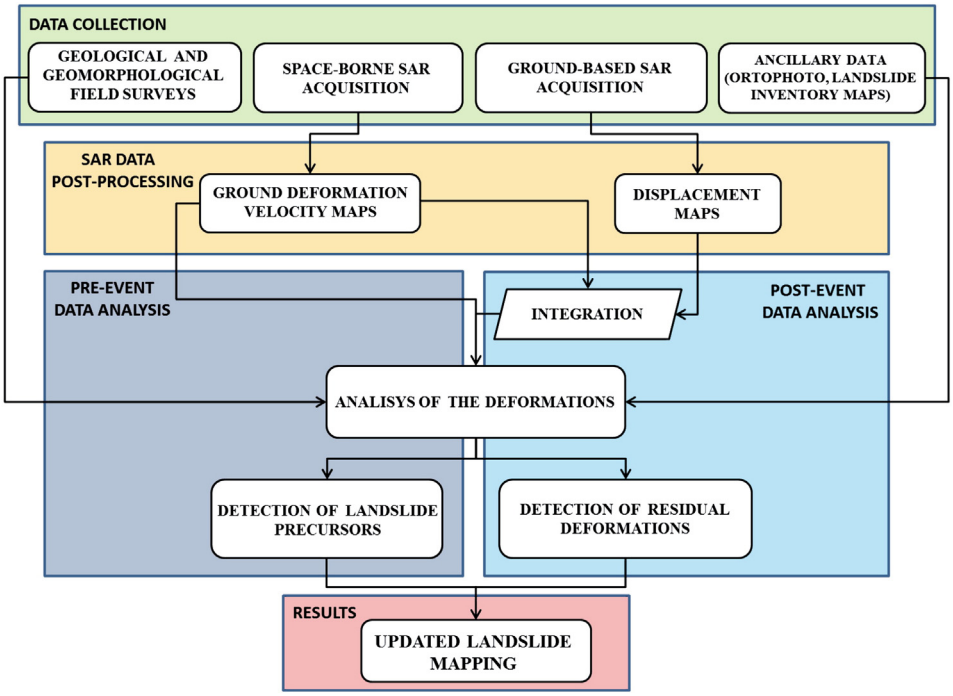

Fig. 7. Flowchart showing the used methodology.

target was to update the landslide limit, to perform a more precise landslide map. The combined use of the space-borne and the ground-based SAR data provided ground displacement measurements with high spatial and temporal accuracy, allowing us to better and more accurately trace the delimitation of the 2010 landslide. Furthermore, the integration of PS- and GB-InSAR approaches allows overcoming their physical limitations. Therefore, in order to compare the results of both techniques, it is possible to study the same area from different points of view and in different temporal intervals.

In order to validate the integration results, the new landslide map resulting from the SAR data integration was qualitatively compared with the field survey results, i.e., the geomorphological map (Fig. 4C), the building damage assessment and the fracture pattern map (Fig. 5).

4. Results

4.1. PSI data

The ground deformation velocity maps were characterized by different PS density and acquisition periods. The ERS 1/2, ENVISAT, and RADARSAT-1 data were acquired during the pre-event phase (1992–2010) with respect to the 2010 landslide and COSMO-SkyMed data were collected during the post-event phase (2011–2012). The PS distribution within the 2010 landslide is not homogeneous; most of the PS are located in correspondence with the buildings of San Fratello, allowing the observation of the ground deformation phenomena along the landslide crown, whereas within the landslide body, the presence of PS is strongly reduced from the absence of reflectors. Each PS is characterized by a V_{los} that can be positive or negative. The first case occurs when the target approaches the sensor along the LOS; on the contrary, negative values characterize PS moving away from the sensor. Projecting PSI data on the downslope direction, only the negative portion of the displacements is emphasized and −2 mm/y is considered the stability threshold value.

4.1.1. ERS 1/2

In Fig. 8, the ground deformation velocity maps, obtained using ERS 1/2 V_{slope} data (1992–2001), are shown in both acquisition orbits. The PS average density is low (Table 1), but it is sufficient to make some observations about the stability of the town of San Fratello. In Fig. 8, it is possible to note that the crown of the 2010 landslide is basically stable, except an area characterized by displacements between −2 and −5 mm/y, emphasized with a red dashed line in the figure; nevertheless very little information can be retrieved about the landslide body. The areas involved in the crowns of the historical landslides of 1754 and 1922 show a residual activity, with average velocities between −2 and more than −20 mm/y (Fig. 8), as highlighted by the V_{slope} maps acquired in ascending and descending orbits (Fig. 8A and B).

4.1.2. ENVISAT and RADARSAT-1

The ground deformation velocity (V_{slope}) maps obtained through the processing of ENVISAT (2003–2010) and RADARSAT-1 (2005–2009) images, acquired in ascending and descending orbits, are shown in Fig. 9. The data obtained by these two satellites were superimposed on the same map because the temporal range of acquisition of RADARSAT-1 data partially overlaps to that of ENVISAT, therefore their results have proven to be useful for a comparison of the measured ground deformations. These maps proved to be more useful with

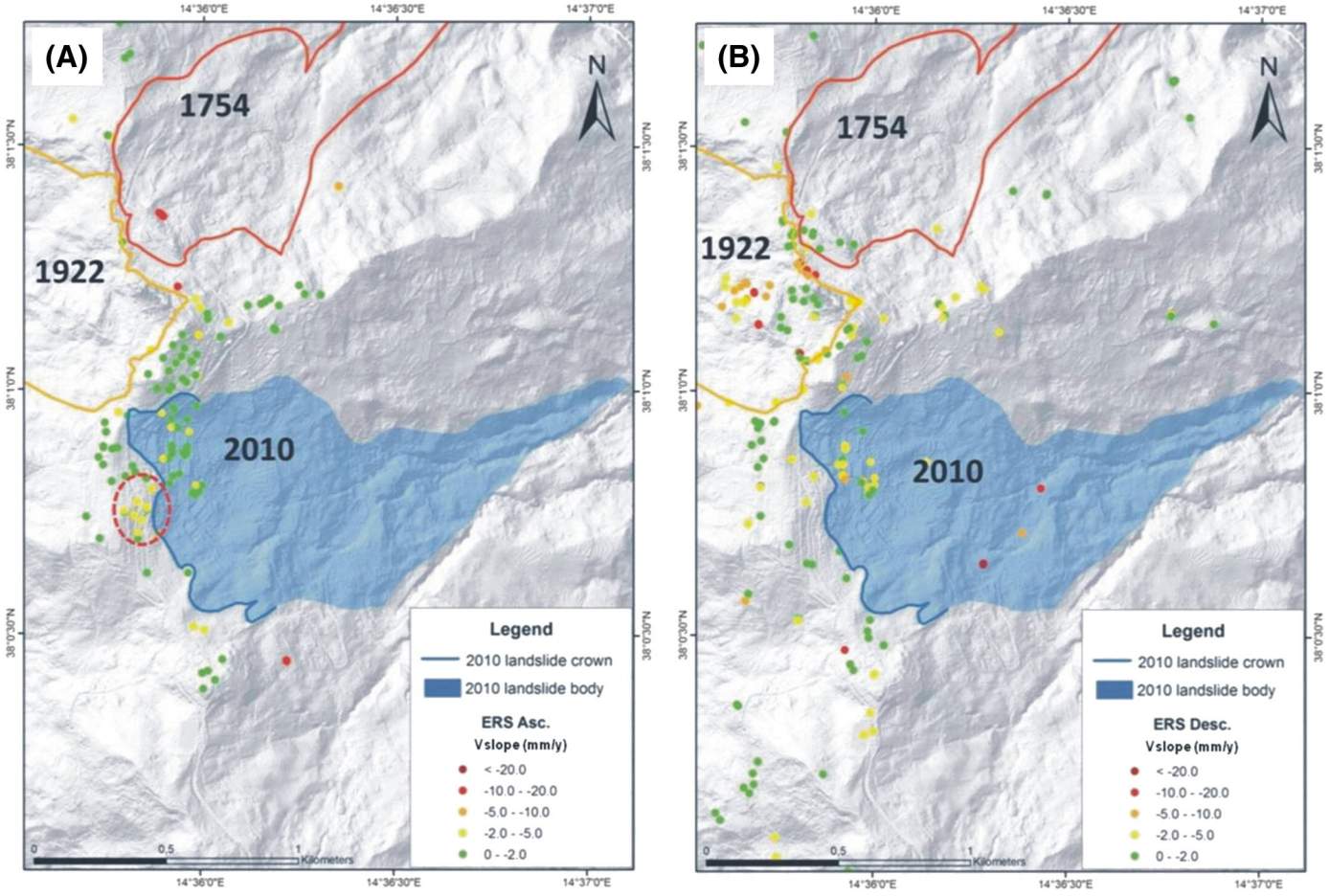

Fig. 8. PS ground deformation velocity maps (V_{slope}), using ERS 1/2, obtained through data acquired in ascending (A) and descending (B) orbits. The areas characterized by higher displacements are emphasized with a red dashed line. (For interpretation of the references to color in this figure legend, the reader is referred to the web version of this article.)

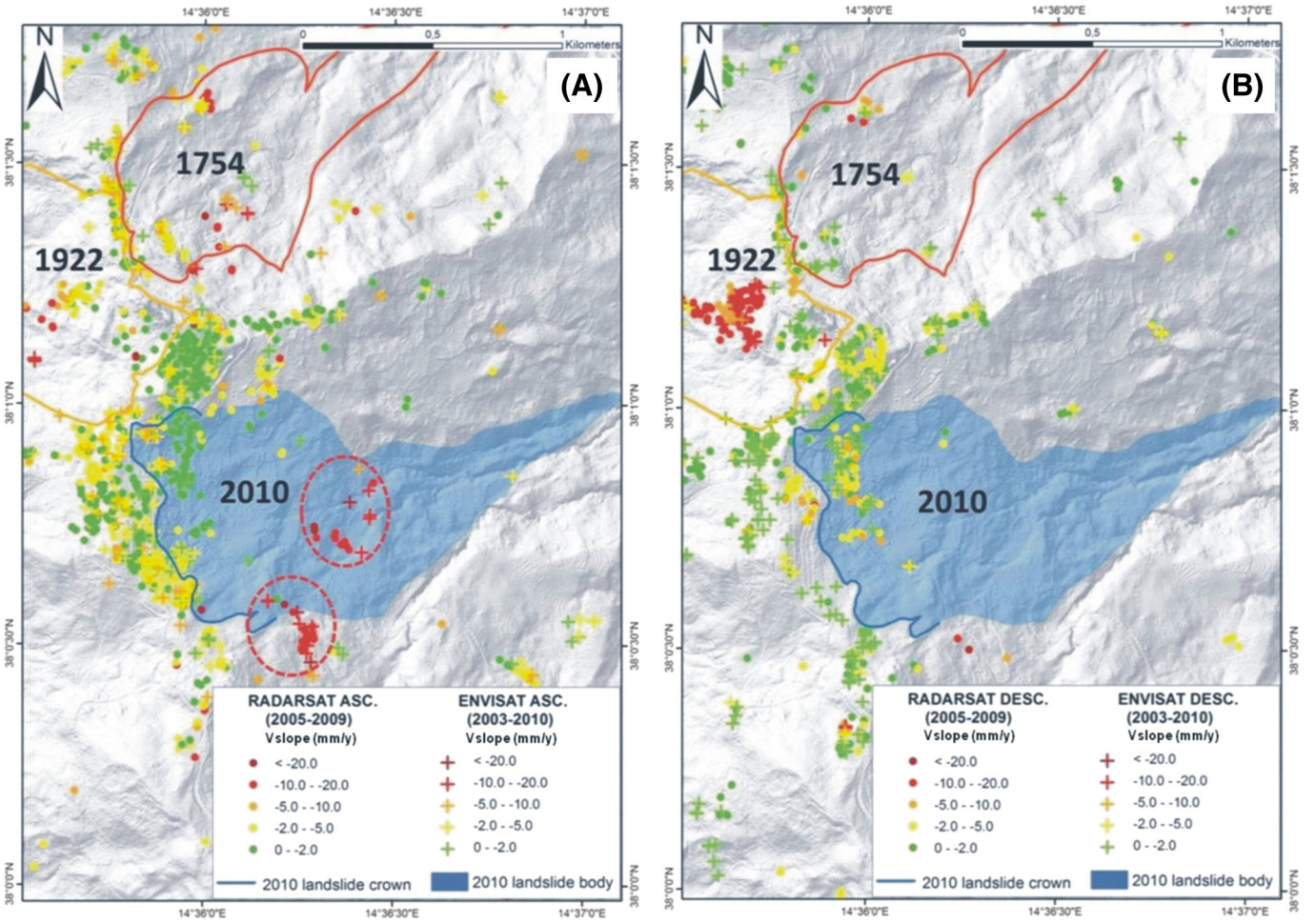

Fig. 9. PS ground deformation velocity maps (V_{slope}), using ENVISAT and RADARSAT-1, obtained through data acquired in ascending (A) and descending (B) orbits. The ENVISAT PSs are shown as crosses, and the RADARSAT are shown as circles. The areas characterized by higher displacements are emphasized with red dashed lines. (For interpretation of the references to color in this figure legend, the reader is referred to the web version of this article.)

respect to those obtained by ERS 1/2 because of their higher PS density (Table 1). In particular, the map obtained using the ascending orbit (Fig. 9A) is characterized by a good density of targets, also within the 2010 landslide body, allowing a better understanding of the pre-event ground deformations affecting the east-facing slope.

The ENVISAT data, indicated with crosses in Fig. 9, show the presence of relevant displacements on the east-facing slope since 2003, more evident in ascending orbit (Fig. 9A) data stacks, where they are characterized by velocities between −5 and more than −20 mm/y (Fig. 9A). Considering the 2010 landslide body, most of the unstable PSs are placed outside the landslide boundary. Data acquired in descending orbit clearly show displacements located on the west-facing slope in the area affected by the 1922 landslide crown (Fig. 9B). Furthermore, several PSs show displacements in correspondence with the 1754 landslide crown (Fig. 9A).

As regards RADARSAT-1 data among the C-band sensors, they are characterized by the highest PS density (Table 1).

According to ENVISAT data, the ascending RADARSAT-1 ones (indicated with circles in Fig. 9A) clearly show within the 2010 landslide body two areas affected by ground deformation that reach velocities ranging from −5 to more than −20 mm/y and that are marked with red dashed lines in Fig. 9A. These data sets are very interesting because the acquisition interval ends a few months before the 2010 landslide. In addition, these maps clearly show deformations in correspondence with the area affected by the 1754 landslide crown (Fig. 9A). The descending data set highlights ground deformation in the 1922 landslide area (Fig. 9B) with velocities between −5 and more than −20 mm/y.

4.1.3. COSMO-SkyMed

The COSMO-SkyMed data were available only in descending orbit; the related ground deformation velocity map (V_{slope}) is shown in Fig. 10. The COSMO-SkyMed data are representative of the 2010 landslide post-event period and are related to a shorter acquisition period (2011–2012) with respect to the other employed satellites. The acquired COSMO-SkyMed ground deformation V_{slope} map is characterized by a higher PS density with respect to those obtained using the C-band sensors, but the PS population is affected by higher velocity standard deviations because of the short acquisition period (1 year).

In particular, Fig. 10 shows the presence of relevant displacements located in the northern part of the 2010 landslide (Stazzone quarter, sector 2 in Fig. 4C). The southern part of the San Fratello town (San Benedetto quarter, sector 4 in Fig. 4C) is also affected by deformation, highlighted by the presence of a cluster of PS showing velocities between −5 and more than −20 mm/y. The qualitative ground validation, based on the damages of buildings and structures, and on the scarps and fractures observed during the field surveys confirms displacement trends according to those registered by the satellite data. The COSMO-SkyMed ground deformation velocity (V_{slope}) map, if compared to those acquired during the pre-event phase, clearly shows that most of the deformation phenomena are located along the 2010 landslide crown; nevertheless evidence of ground displacement is also present in the landslide body. These more recent satellite data continue to show the presence of deformation phenomena located in correspondence with the 1754 landslide crown, according to the C-band satellite data. Information about the 1922 landslide displacements is spatially

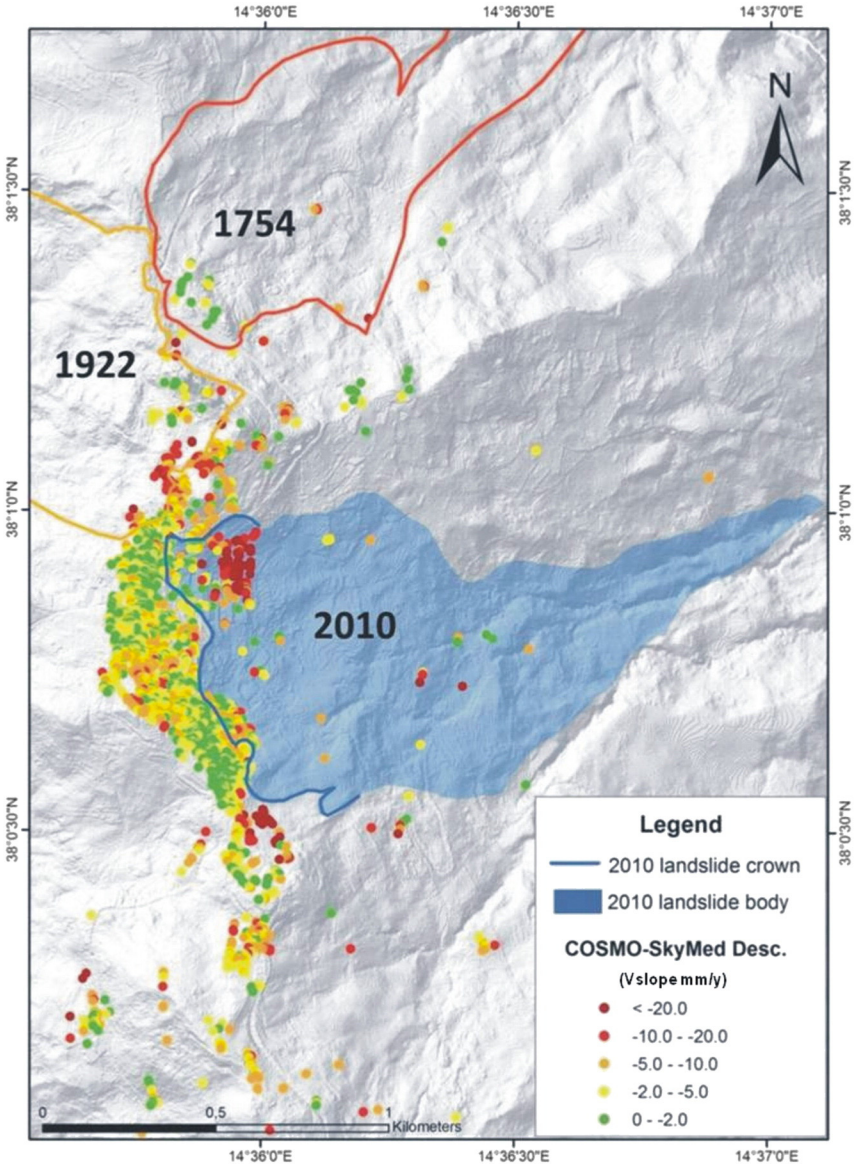

Fig. 10. PS ground deformation velocity map (V_{slope}), using COSMO-SkyMed, obtained by data acquired in descending orbit.

reduced because the town of San Fratello is located along the western boundary of the used COSMO-SkyMed SAR scenes. Nevertheless, in this area deformation velocities, >−20 mm/y, were detected between 2011 and 2012 along the crown of the 1922 landslide (Fig. 10). However, correspondence is good between the damages to buildings and structures and the evidence of movements observed during the field surveys and the ground deformation recorded by the COSMO-SkyMed data (Figs. 4C and 5).

4.2. GB-InSAR data

During the monitoring campaign (10 March 2010–14 March 2013), GB-InSAR data such as cumulative displacement maps were produced as well as displacement time series of some representative points selected prevalently on the town area for civil protection purposes. The collected displacement maps are shown in Fig. 11 with a color scale visualizing (i) stable areas in green; (ii) sectors characterized by light displacements (between about 50 and 300 mm) with colors ranging from yellow to red; and (iii) sectors characterized by the highest monitored displacement in purple (from light to dark tones). The logistic of the GB-InSAR system installation favored a good spatial coverage of the data on the monitored area, especially with regard to the Stazzone, Riana, San Benedetto, and Porcaro quarters (located as shown in Fig. 4C). Nevertheless, shadowing effects caused by the ridge divide, hide part of the western town area from the radar scene; counterslope surfaces cause the same effect in correspondence with some eastern slope sectors, so that in these areas no GB-InSAR data are available, as it is possible to observe in Fig. 11. According to the collected cumulative displacement maps, the peak deformations within the monitored area (dashed ovals in Fig. 11D) are located in correspondence with the San Benedetto (2294 mm) and Porcaro quarters (2178 mm); whereas in correspondence with the Stazzone and Riana quarters, ground deformations reached 604 and 545 mm, respectively.

Displacement time series were also extracted on the displacement maps of 10 control points, selected in correspondence with areas where the radar signal is characterized by high stability, high signal/noise ratio, and high power and coherence parameters to accurately monitor the deformations of structures and buildings (Fig. 11E). The control points selected in correspondence with the Stazzone quarter (P1, P2, P3, P4) record cumulative displacements between 15 (P1) and 226 mm (P3); whereas in the Riana quarter (P5, P6, P7, P8), they range from 86 (P5) to 321 mm (P7). The peak displacements are

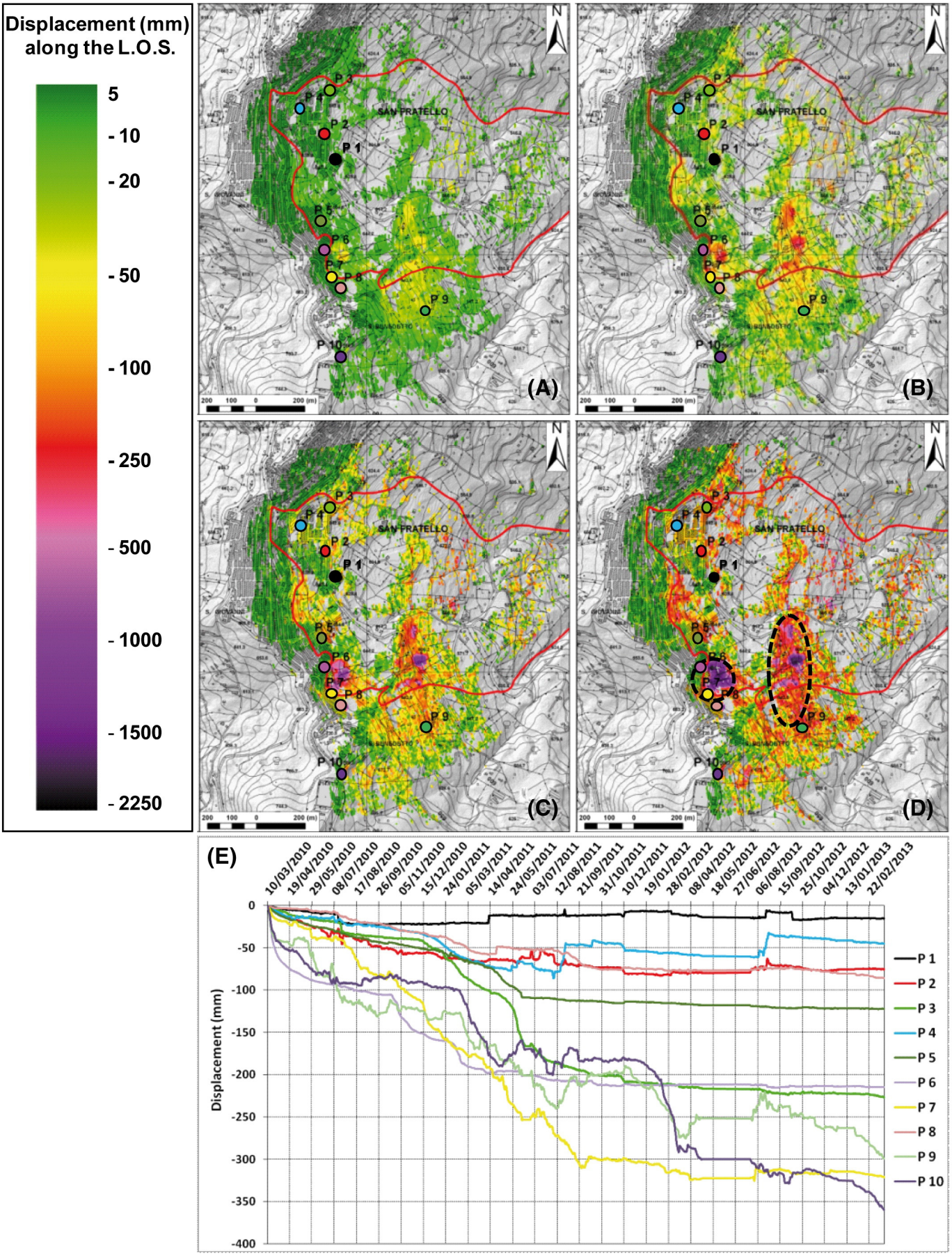
Displacement (mm) along the L.O.S.
5
- 10
- 20
- 50
- 100
- 250
- 500
- 1000
- 1500
- 2250
SAN FRATELLO
P 1
P 2
P 3
P 4
P 5
P 6
P 7
P 8
P 9
P 10
(A)
(B)
(C)
(D)
(E)
Displacement (mm)
0
-50
-100
-150
-200
-250
-300
-350
-400
10/03/2010
19/04/2010
29/05/2010
08/07/2010
17/08/2010
26/09/2010
05/11/2010
15/12/2010
24/01/2011
05/03/2011
14/04/2011
24/05/2011
03/07/2011
12/08/2011
21/09/2011
31/10/2011
10/12/2011
19/01/2012
28/02/2012
08/04/2012
18/05/2012
27/06/2012
06/08/2012
15/09/2012
25/10/2012
04/12/2012
13/01/2013
22/02/2013

recorded in the Porcaro (P9 = 299 mm) and San Benedetto quarters (P10 = 360 mm). The displacements recorded in correspondence with the control points are related to their specific location, thus they do not necessarily reflect the maximum displacement of the whole investigated area (Fig. 11).

5. Discussion

On 14 February 2010, a complex landslide occurred along the eastern slope of the San Fratello town. In this paper, space-borne and ground-based InSAR data were analyzed and integrated to perform a more accurate delimitation of the landslide.

Space-borne InSAR techniques are useful to monitor unstable areas only under specific conditions: the main limitations related to its applicability regard the revisiting time, the slope exposure with respect to the satellite LOS, and the velocity of the investigated movements. Nevertheless, the space-borne InSAR technique ability of measuring very slow and gradual ground displacements (up to few millimeters per year) represents a valuable support to landslide hazard prevention activities, giving the opportunity to detect extremely slow movements that usually occur several weeks or months before the catastrophic failure, preceding major landslide disasters as highlighted by ENVISAT and RADARSAT-1 data.

On the other hand, GB-InSAR allows a continuous monitoring of the displacements from few millimeters per day up to 1 or more meters per day over unstable areas. Furthermore, the instrument versatility enables the investigation of very steep unstable slope not visible from the satellite, and it permits us to choose the best LOS. These characteristics make this technique particularly useful for emergency phases.

Information about ground deformation, obtained using the GB-InSAR technique, can be refined when combined with space-borne InSAR data.

As regard the San Fratello landside, the GB-InSAR instrument was installed on the facing slope of the landslide: this location represents the best solution considering the geomorphology of the area. The distance is quite high, and this can determine noise, especially where the cross range resolution is lower. The presence of wide vegetation cover, on the interested slope, limits the possibility to investigate the whole landslide area. Only the portion of the landslide that involves the village can be analyzed because the housing and infrastructure represent good reflectors for radar monitoring. This problem can be solved using the space-borne SAR data, which allow the observation of the higher part of the study area nonvisible to the GB-InSAR.

The combined space-borne and ground-based InSAR analysis was performed in order to monitor the evolution of the 2010 landslide and to manage the post-emergency phase. With respect to the 2010 landslide geomorphological map (Fig. 4C), the analysis of the available SAR data enhanced areas affected by ground deformations also outside the surveyed landslide perimeter, showing that the latter was slightly underestimated.

The PSI data projected along the downslope direction, which is quite similar to the GB-InSAR LOS, that confirm the presence of widespread slope instability in the area, not only in correspondence with the 2010 landslide: ground deformations within two large areas, but also in correspondence with the two historical landslide crowns (1754 and 1922) are also detected (Figs. 8, 9, and 10).

As regards the 2010 landslide, ground deformation velocity maps obtained through PSI projected data (V_{slope}), acquired since 1992, allowed highlighting the occurrence of ground displacements during the pre-event phase and identifying eventual displacements in the post-emergency phase related to the landslide.

In particular, between the 1992 and 2001 (ERS 1/2 acquisition period), no important deformations were detected; whereas ENVISAT and RADARSAT-1 ground deformation velocity maps (V_{slope}) highlight the occurrence of displacements between the 2003 and the beginning of the 2010. During this period, the landslide crown area was characterized by stability, and an area characterized by ground deformation velocities higher than −20 mm/y is located on the landslide body, partially outside the DRPC boundary, performed by Pino et al., 2010 (Fig. 4C). This latter area was intensely damaged on 14 February 2010. Unfortunately, no evidence of displacements can be retrieved in correspondence with the landslide toe because of the lack of PS, owing to the intense vegetation cover. These results are in agreement with the landslide evolution trend, which was characterized by a retrogressive behavior: indeed, the pre-event data (ERS 1/2, ENVISAT, and RADARSAT) show the major displacements in the body area and the minor in the crown area. Observing in sequence ERS 1/2, ENVISAT, and RADARSAT data, an increase of ground deformation velocities in the crown area that became more marked in the post-event data, was observed. This is in agreement with the cumulated GB-InSAR displacements.

The PSI data acquired between 2003 and 2010 were useful to highlight the potential risk of the area, but their distribution could not be used to forecast the possible 14 February 2010 landslide spatial extent.

Considering the post-event available PSI data, COSMO-SkyMed ones were very useful to refine the 2010 landslide crown boundary. The higher PS density allowed us to detect a high number of targets in correspondence with the town area; several buildings located outside the DRPC landslide boundary (Pino et al., 2010) showed deformations. The presence of areas affected by ground deformation along the crown can be related to the higher X-band sensibility in the detection of displacements and/or to the retrogression of the landslide, which continued after 14 February 2010, affecting part of the town not severely involved in the event. The most interesting results were obtained in the western sector of the San Benedetto quarter, which was not initially damaged by the landslide. Here field-surveyed fractures and building damages started to develop from 2011, as confirmed by COSMO-SkyMed data. However, other buildings affected by deformation are also located outside the DRPC boundary, also in the Riana quarter and north of the Stazzone quarter, confirming the need to refine the landslide boundary crown.

The GB-InSAR monitoring, carried out during the post-2010 landslide event phase, provided the monitoring of the related displacement pattern evolution. The GB-InSAR data also proved to be very useful to confirm the results obtained through COSMO-SkyMed ground deformation velocity map (V_{slope}), given its temporal coverage with the latter PSI data. In Fig. 12, the GB-InSAR cumulative displacement map (from March 2010 to March 2013) is shown together with the COSMO-SkyMed V_{slope}, whose acquisition period partially corresponds to the GB-InSAR period (May 2011–May 2012). On the map (Fig. 12), it is also possible to observe the proposed new landslide boundary. The cumulative displacement map highlights that the higher ground deformations (up to 2.3 m) took place in correspondence with the San Benedetto-Riana quarters (Fig. 12). Furthermore, a widespread area affected by ground deformation is detected in correspondence with the Porcaro quarter and north of the Stazzone quarter. The above-mentioned areas are partially located outside the DRPC landslide boundary (Pino et al., 2010).

The use of the GB-InSAR cumulative displacement maps proved their usefulness also to recognize the areas affected by the most important residual risk, which are placed in correspondence with the Porcaro and San Benedetto quarters. Considerable deformation can be assessed also in the Stazzone and Riana quarters confirming the instability of the

Fig. 11. San Fratello landslide cumulative displacement maps: (A) 2010; (B) 2010; (C) 2011; and (D) 2012. Dashed ovals represent the areas affected by the peak displacements; P1–10 stand for the location of the control points. (E) Time series of the selected control points. (For interpretation of the references to color in this figure, the reader is referred to the web version of this article.)

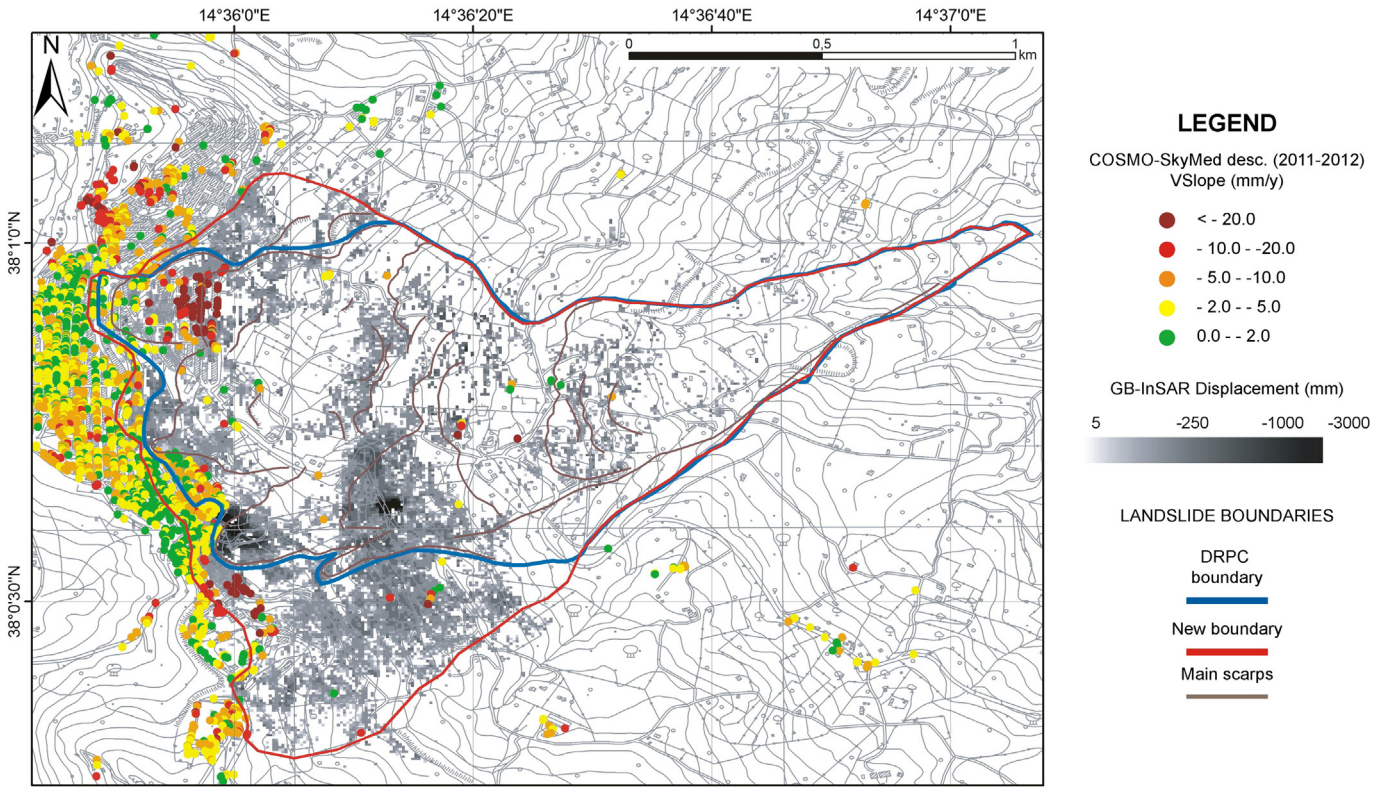

Fig. 12. Comparison between the DRPC (Pino et al., 2010) and the new boundary inferred by the integration between PSI and GB-InSAR data. On the background: the GB-InSAR cumulative displacement map (from March 2010 to March 2013) and the COSMO SkyMed V_{slope} data, together with the main scarp pattern.

crown area during the post-event phase and the retrogressive behavior of the mass movement.

The extension of the landslide boundaries is confirmed by the spatial distribution of the damages of buildings and infrastructures. In particular, in Fig. 12 it is possible to observe how the main scarps delineate areas affected by major displacements, also recognized by the SAR data (Fig. 12). The new boundary determines a new estimation of the landslide area, from 1 to 1.2 km^2.

Considering the historical landslides, the space-borne multisensor approach allowed the detection of deformation phenomena located along the crown of the 1922 landslide. This instability was observed since the beginning of the ERS 1/2 acquisition (1992–2001) and continues today passing from −9 mm/y to more than −20 mm/y recorded by COSMO-SkyMed.

6. Conclusions

The integration between PS and GB-InSAR data, applied to the 2010 landslide in San Fratello test site, allowed us to analyze the landslide displacements in different time intervals and with different LOS and ground resolutions for a period spanning between 1992 and 2013.

This multisensor approach was employed in order to improve the 2010 landslide boundary obtained through geomorphological mapping and performed immediately after the event. The new boundary considers the areas affected by ground deformation, detected by the C-band sensors (ERS1/2, ENVISAT, and RADARSAT-1), and the areas characterized by slope instability, highlighted during the post-event phase by the X-band COSMO-SkyMed satellite and by the GB-InSAR system located inside and outside the previous limits.

In order to better compare space-borne data with the GB-InSAR data, satellite data were projected in the downslope direction that is quite similar to the GB-InSAR LOS direction.

In this work, the combined use of GB-InSAR and PSI techniques was applied to improve the capacity of the monitoring system of slow-moving landslides. Results prove the usefulness of this methodology to accurately map and monitor the area affected by ground deformation. The GB-InSAR, coupled with traditional and innovative space-borne SAR, allowed for the production of maps benefitting from the different spatial and temporal resolutions of the radar sensors. The PSI data were used primarily to perform regional scale investigations for the detection of unstable areas and for the assessment of the long-term behavior of the considered landslide. The GB-InSAR system was used in a specific area of interest, improving the spatial resolution of the measurement and reducing the revisiting time.

The obtained accuracy in mapping and in monitoring an area subjected to mass movement is fundamental in risk management and in preparation of emergency plans.

Acknowledgments

The research leading to these results received funding from the European Union Seventh Framework Program (FP7/2007–2013) under grant agreement No. 242212 (Project DORIS). This study was founded by the Seventh Framework Program of European Commission: Landslide Modelling and Tools for vulnerability assessment preparedness and recovery management (LAMPRE).

We thank five anonymous reviewers and the editor Richard A. Marston for their suggestions which greatly improved this work.

References

Antonello, G., Casagli, N., Farina, P., Leva, D., Nico, G., Sieber, A.J., Tarchi, D., 2004. Ground-based SAR interferometry for monitoring mass movements. Landslide 1, 21–28.

Atzori, P., Vezzani, L., 1974. Lineamenti petrografico-strutturali della catena peloritana. Geol. Romana 13, 21–27.

Atzori, P., Ghisetti, F., Pezzino, A., Vezzani, L., 1978. Strutture ed evoluzione geodinamica recente dell'area peloritana (Sicilia nord-orientale). Boll. Soc. Geol. Ital. 97, 31–56.

Bamler, R., Hartl, P., 1998. Synthetic aperture radar interferometry. Inverse Probl. 14, 1–54.

Bellotti, F., Bianchi, M., Colombo, D., Ferretti, A., Tamburini, A., 2014. Advanced InSAR techniques to support landslide monitoring. In: Pardo-Igúzquiza, E., Guardiola-Albert, C., Heredia, J., Moreno-Merino, L., Durán, J.J., Vargas-Guzmán, J.A. (Eds.), Mathematics of Planet Earth, Lecture Notes in Earth System Sciences. Springer, Berlin Heidelberg, pp. 287–290.

Bianchini, S., Cigna, F., Righini, G., Proietti, C., Casagli, N., 2012. Landslide hotspot mapping by means of persistent scatterer interferometry. Environ. Earth Sci. 67 (4), 1155–1172.

Bianchini, S., Herrera, G., Mateos, R.M., Davide Notti, D., Garcia, I., Mora, O., Moretti, S., 2013. Landslide activity maps generation by means of persistent scatterer interferometry. Remote Sens. 5 (12), 6198–6222. http://dx.doi.org/10.3390/rs5126198.

Bianchini, S., Ciampalini, A., Raspini, F., Bardi, F., Di Traglia, F., Moretti, S., Casagli, N., 2014. Multi-temporal evaluation of landslide movements and impacts on buildings in San Fratello (Italy) by means of C-band and X-band PSI data. Pure Appl. Geophys. http://dx.doi.org/10.1007/s00024-014-0839-2.

Bovenga, F., Wasowski, J., Nitti, D.O., Nutricato, R., Chiaradia, M.T., 2012. Using COSMO-SkyMed X-band and ENVISAT C-band SAR interferometry for landslides analysis. Remote Sens. Environ. 119, 272–285.

Casagli, N., Farina, P., Leva, D., Nico, G., Tarchi, D., 2002. Monitoring the Tessina landslide by a ground-based interferometer and assessment of the system accuracy. Proceedings of the International Geoscience and Remote Sensing Symposium (IGARSS), Toronto, Canada, pp. 2915–2917.

Casagli, N., Tibaldi, A., Merri, A., Del Ventisette, C., Apuani, T., Guerri, L., Fortuny-Guasch, J., Tarchi, D., 2009. Deformation of Stromboli Volcano (Italy) during the 2007 eruption revealed by radar interferometry, numerical modelling and structural geological field data. J. Volcanol. Geotherm. Res. 182, 182–200.

Casagli, N., Catani, F., Del Ventisette, C., Luzi, G., 2010. Monitoring, prediction, and early warning using ground-based radar interferometry. Landslides 7, 291–301.

Ciampalini, A., Cigna, F., Del Ventisette, C., Moretti, S., Liguori, V., Casagli, N., 2012. Integrated geomorphological mapping in the north-western sector of Agrigento (Italy). J. Maps 8 (2), 136–145.

Ciampalini, A., Bardi, F., Bianchini, S., Frodella, W., Del Ventisette, C., Moretti, S., Casagli, N., 2014. Analysis of building deformation in landslide area using multisensor PSInSAR™ technique. Int. J. Appl. Earth Obs. Geoinform. 33, 166–180.

Cigna, F., Del Ventisette, C., Liguori, V., Casagli, N., 2011. Advanced radar-interpretation of InSAR time series for mapping and characterization of geological processes. Nat. Hazards Earth Syst. Sci. 11, 865–881.

Cigna, F., Del Ventisette, C., Gigli, G., Menna, F., Agili, F., Liguori, V., Casagli, N., 2012. Ground instability in the old town of Agrigento (Italy) depicted by on-site investigations and Persistent Scatterers data. Nat. Hazards Earth Syst. Sci. 12, 3589–3603.

Colesanti, C., Wasowski, J., 2006. Investigating landslides with space-borne Synthetic Aperture Radar (SAR) interferometry. Eng. Geol. 88, 173–199.

Colesanti, C., Ferretti, A., Prati, C., Rocca, F., 2003. Monitoring landslides and tectonic motion with the Permanent Scatterers technique. Eng. Geol. 68, 3–14.

Corsini, A., Farina, P., Antonello, G., Barbieri, M., Casagli, N., Coren, F., Guerri, L., Ronchetti, F., Sterzai, P., Tarchi, D., 2006. Space-borne and ground-based SAR interferometry as tools for landslide hazard management in civil protection. Int. J. Remote Sens. 27 (12), 2351–2369.

Crosetto, M., Crippa, B., Biescas, E., 2005. Early detection and in-depth analysis of deformation phenomena by radar interferometry. Eng. Geol. 79 (1–2), 81–91.

Crosetto, M., Monserrat, O., Iglesias, R., Crippa, B., 2010. Persistent scatterer interferometry: potential, limits and initial C- and X-band comparison. Photogramm. Eng. Remote Sens. 76 (9), 1061–1069.

Crosetto, M., Monserrat, O., Cuevas, M., Crippa, B., 2011. Spaceborne differential SAR interferometry: data analysis tools for deformation measurement. Remote Sens. 3, 305–318.

Del Ventisette, C., Intrieri, E., Luzi, G., Casagli, N., Fanti, R., Leva, D., 2011. Using ground based radar interferometry during emergency: the case of the A3 motorway (Calabria Region, Italy) threatened by a landslide. Nat. Hazard Heart Syst. Sci. 11, 2483–2495.

Del Ventisette, C., Casagli, N., Fortuny-Guasch, J., Tarchi, D., 2012a. Ruinon landslide (Valfurva, Italy) activity in relation to rainfall by means of GBInSAR monitoring. Landslides 9 (4), 497–509.

Del Ventisette, C., Garfagnoli, F., Ciampalini, A., Battistini, A., Gigli, G., Moretti, S., Casagli, N., 2012b. An integrated approach to the study of catastrophic debris-flows: geological hazard and human influence. Nat. Hazards Earth Syst. Sci. 12, 2907–2922.

Del Ventisette, C., Ciampalini, A., Manunta, M., Calò, F., Paglia, L., Ardizzone, F., Mondini, A.C., Reichembach, P., Mateos, R.M., Bianchini, S., Garcia, I., Füsi, B., Deak, Z.V., Radi, K., Graniczny, M., Kowalski, Z., Piatkowska, A., Przylucka, M., Retzo, H., Strozzi, T., Colombo, D., Mora, O., Sanches, F., Herrera, G., Moretti, S., Casagli, S., Guzzetti, F., 2013. Exploitation of large archives of ERS and ENVISAT C-band SAR data to characterize ground deformations. Remote Sens. 5 (8), 3896–3917.

Di Traglia, F., Del Ventisette, C., Mugnai, F., Intrieri, E., Rosi, M., Moretti, S., Casagli, N., 2013. Ground based InSAR reveals conduit pressurization pulses at Stromboli volcano. Terra Nova 25, 192–198.

Farina, P., Moretti, S., Colombo, D., Fumagalli, A., Manunta, P., 2004. Landslide risk analysis by means of remote sensing techniques: results from the ESA SLAM project. Int. Geosci. Remote Sens. Symp. (IGARSS) 1, 62–65.

Ferretti, A., Prati, C., Rocca, F., 2000. Non-linear subsidence rate estimation using permanent scatterers in differential SAR interferometry. IEEE Trans. Geosci. Remote Sens. 38 (5), 2202–2212.

Ferretti, A., Prati, C., Rocca, F., 2001. Permanent scatterers in SAR interferometry. IEEE Trans. Geosci. Remote Sens. 39 (1), 8–20.

Ferretti, A., Bianchi, M., Prati, C., Rocca, F., 2005. Higher-order permanent scatterers analysis. Eurasip J. Appl. Signal Process. 20, 3231–3242.

Ferretti, A., Fumagalli, A., Novali, F., Prati, C., Rocca, F., Rucci, A., 2011. A new algorithm for processing interferometric data-stacks: SqueeSAR. IEEE Trans. Geosci. Remote Sens. 49 (9), 3460–3470.

Finetti, I., Lentini, F., Carbone, S., Catalano, S., Del Ben, A., 1996. Il sistema Appennino meridionale-Arco Calabro-Sicilia nel Mediterraneo centrale: studio geologico-geofisico. Boll. Soc. Geol. Ital. 115, 529–559.

Frattini, P., Crosta, G.B., Allievi, J., 2013. Damage to buildings in large slope rock instabilities monitored with the PSInSAR™ technique. Remote sensing, special issue: remote sensing for landslides investigation: from research into practice. 5 (10), 4753–4773.

Gigli, G., Fanti, R., Canuti, P., Casagli, N., 2011. Integration of advanced monitoring and numerical modeling techniques for the complete risk scenario analysis of rockslides: the case of Mt. Beni (Florence, Italy). Eng. Geol. 120, 48–59.

Guzzetti, F., Mondini, A.C., Cardinali, M., Fiorucci, F., Santangelo, M., Chang, K.T., 2012. Landslide inventory maps: new tools for an old problem. Earth Sci. Rev. 112, 42–66.

Hanssen, R.S., 2005. Satellite radar interferometry for deformation monitoring: a priori assessment of feasibility and accuracy. Int. J. Appl. Earth Obs. Geoinform. 6, 253–260.

Herrera, G., Fernández-Merodo, J.A., Mulas, J., Pastor, M., Luzi, G., Monserrat, O., 2009. A landslide forecasting model using ground based SAR data: the Portalet case study. Eng. Geol. 105, 220–230.

Herrera, G., Gutiérrez, F., García-Davalillo, J.C., Guerrero, J., Notti, D., Galve, J.P., Fernández-Merodo, J.A., Cooksley, G., 2013. Multi-sensor advanced DInSAR monitoring of very slow landslides: the Tena Valley case study (Central Spanish Pyrenees). Remote Sens. Environ. 128, 31–43.

Intrieri, E., Di Traglia, F., Del Ventisette, C., Gigli, G., Mugnai, F., Luzi, G., Casagli, N., 2013. Flank instability of Stromboli volcano (Aeolian Islands, Southern Italy): integration of GB-InSAR and geomorphological observations. Geomorphology 201, 60–69.

Lentini, F., Vezzani, L., 1975. Le Unità mesozoiche della copertura sedimentaria del basamento cristallino peloritano (Sicilia nord-orientale). Boll. Soc. Geol. Ital. 94, 537–554.

Lentini, F., Carbone, S., Catalano, S., Grasso, M., Monaco, C., 1990. Principali elementi strutturali del thrust belt appenninico-maghrebide in Sicilia centro-orientale. Mem. Soc. Geol. Ital. 45, 495–502.

Lentini, F., Carbone, S., Catalano, S., 1994. Main structural domains of the central Mediterranean region and their tectonic evolution. Boll. Geofis. Teor. Appl. 36 (141–144), 103–125.

Lentini, F., Carbone, S., Catalano, S., Grasso, M., 1995. Principali lineamenti strutturali della Sicilia nord-orientale. Studi Geol. Camerti Vol. Spec. 1995/2, 319–329.

Lentini, F., Catalano, S., Carbone, S., 2000. Carta Geologica della provincia di Messina scala 1:50.000. S.EL.CA., Firenze.

Luzi, G., Pieraccini, M., Mecatti, D., Noferini, L., Guidi, G., Moia, F., Atzeni, C., 2004. Ground-based radar interferometry for landslides monitoring: atmospheric and instrumental decorrelation sources on experimental data. IEEE Trans. Geosci. Remote Sens. 42 (11), 2454–2466.

Luzi, G., Monserrat, O., Crosetto, M., Copons, R., Altimir, J., 2010. Ground-based SAR interferometry applied to landslide monitoring in mountainous areas. Mountain Risks Conference: Bringing Science to Society, Firenze, Italy, pp. 24–26.

Massonnet, D., Feigl, K.L., 1998. Radar interferometry and its application to changes in the Earth's surface. Rev. Geophys. 36, 441–500.

Meisina, C., Zucca, F., Notti, D., Colombo, A., Cucchi, A., Savio, G., Giannico, C., Bianchi, M., 2008. Geological interpretation of PSInSAR data at regional scale. Sensors 8, 7469–7492 (ISSN 1424-8220).

Meisina, C., Notti, D., Zucca, F., Ceriani, M., Colombo, A., Poggi, F., Roccati, A., Zaccone, A., 2013. The use of PSInSAR™ and SqueeSAR™ techniques for updating landslide inventories. In: Margottini, C., Canuti, P., Sassa, K. (Eds.), Landslide Science and Practice. Springer, Berlin Heidelberg, pp. 81–87.

Noferini, L., Pieraccini, M., Mecatti, D., Macaluso, G., Atzeni, C., Mantovani, M., Marcato, G., Pasuto, A., Silvano, S., Tagliavini, F., 2007. Using GB-SAR technique to monitor slow moving landslide. Eng. Geol. 95, 88–98.

Noferini, L., Takayama, T., Student Member, I.E.E.E., Pieraccini, M., Mecatti, D., Macaluso, G., Luzi, G., Atzeni, C., 2008. Analysis of ground-based SAR data with diverse temporal baselines. IEEE Trans. Geosci. Remote Sens. 46, 6.

Ogniben, L., 1960. Nota illustrativa dello schema geologico della Sicilia nord-orientale. Riv. Min. Sicil. 11 (64–65), 183–212.

PAI—Piano Stralcio di Bacino per l'Assetto Idrogeologico, 2010. AdB Regione Sicilia. http://www.sitr.regione.sicilia.it/pai.

Pieraccini, M., Tarchi, D., Rudolf, H., Leva, D., Luzi, G., Atzeni, C., 2000a. Interferometric radar for remote monitoring of building deformations. Electron. Lett. 36 (6), 569–570.

Pieraccini, M., Tarchi, D., Rudolf, H., Leva, D., Luzi, G., Bartoli, G., Atzeni, C., 2000b. Structural static testing by interferometric synthetic radar. NDTandE Intl. 33 (8), 565–570.

Pieraccini, M., Casagli, N., Luzi, G., Tarchi, D., Mecatti, D., Noferini, L., Atzeni, C., 2003. Landslide monitoring by ground-based radar interferometry: a field test in Valdarno (Italy). Int. J. Remote Sens. 24 (6), 1385–1391.

Pino, P., Cotone, S., Quattrocchi, S., 2010. Carta geomorfologica della frana di San Fratello. Dipartimento Regionale della Protezione Civile Regione Siciliana.

Pulvirenti, L., Chini, M., Pierdicca, N., Guerriero, L., Ferrazzoli, P., 2011. Flood monitoring using multi-temporal COSMO-SkyMed data: image segmentation and signature interpretation. Remote Sens. Environ. 115, 990–1002.

Raspini, F., Cigna, F., Moretti, S., 2012. Multi-temporal mapping of land subsidence at basin scale exploiting persistent scatterer interferometry: case study of Gioia Tauro plain (Italy). J. Maps 8, 514–524.

Raspini, F., Moretti, S., Casagli, N., 2013. Landslide mapping using SqueeSAR data: Giampilieri (Italy) case study. In: Margottini, C., Canuti, P., Sassa, K. (Eds.), Landslide Science and Practice. Springer, Berlin Heidelberg, pp. 147–154.

Raucoules, D., Parcharidis, I., Feurer, D., Novali, F., Ferretti, A., Carnec, C., Lagios, E., Sakkas, V., Le Mouelic, S., Cooksley, G., Hosford, S., 2008. Ground deformation detection of the greater area of Thessaloniki (Northern Greece) using radar interferometry techniques. Nat. Hazards Earth Syst. Sci. 8 (4), 779–788.

Righini, G., Pancioli, V., Casagli, N., 2012. Updating landslide inventory maps using Persistent Scatterer Interferometry (PSI). Int. J. Remote Sens. 33, 2068–2096.

Singhroy, V., Mattar, K., Gray, L., 1998. Landslide characterization in Canada using interferometric SAR and combined SAR and TM images. Adv. Space Res. 2 (3), 465–476.
Tapete, D., Fanti, R., Cecchi, R., Petrangeli, P., Casagli, N., 2012. Satellite radar interferometry for monitoring and early-stage warning of structural instability in archaeological sites. J. Geophys. Eng. 9, S10–S25.
Tarchi, D., Ohlmer, E., Sieber, A.J., 1997. Monitoring of structural changes by radar interferometry. Res. Nondestruct. Eval. 9, 213–225.
Tarchi, D., Rudolf, H., Pieraccini, M., Atzeni, C., 2000. Remote monitoring of buildings using a ground-based SAR: application to cultural heritage survey. Int. J. Remote Sens. 21 (18), 3545–3551.
Tarchi, D., Casagli, N., Moretti, S., Leva, D., Sieber, A.J., 2003a. Monitoring landslide displacements by using ground-based radar interferometry: application to the Ruinon landslide in the Italian Alps. J. Geophys. Res. 108 (B8–2387), 101–114.
Tarchi, D., Casagli, N., Fanti, R., Leva, D., Luzi, G., Pasuto, A., Pieraccini, M., Silvano, S., 2003b. Landslide monitoring by using ground-based SAR interferometry: an example of application to the Tessina landslide in Italy. Eng. Geol. 68, 15–30.
Zhao, C., Lu, Z., Zhang, Q., De La Fuente, J., 2012. Large-area detection and monitoring with ALOS/PALSAR imagery data over Northern California and Southern Oregon, USA. Remote Sens. Environ. 124, 348–359.